



Published in final edited form as:

Ophthalmol Retina. 2018 June ; 2(6): 587–598. doi:10.1016/j.oret.2017.10.008.

Fluorescence Lifetime Imaging Ophthalmoscopy: A Novel Way to Assess Macular Telangiectasia Type 2

Lydia Sauer^{1,2}, Rebekah H. Gensure¹, Martin Hammer², and Paul S. Bernstein^{1,3}

¹John A. Moran Eye Center, University of Utah, Salt Lake City, UT, USA

²University Hospital Jena, Bachstraße 18, 07743, Jena, Germany

Abstract

Purpose—Macular Telangiectasia Type 2 (MacTel) is an uncommon, late-onset complex retinal disease that leads to central vision loss. No causative gene(s) have been identified so far, resulting in a challenging clinical diagnostic dilemma because retinal changes of early stages are often subtle. The objective of this study was to investigate the benefit of fluorescence lifetime imaging ophthalmoscopy (FLIO) for retinal imaging in patients with MacTel.

Design—Cross-sectional study from a tertiary-care retinal referral practice.

Subjects and Controls—42 eyes of 21 patients (mean age 60.5 ± 13.3 years) with MacTel as well as an age-matched healthy control group (42 eyes of 25 subjects, mean age 60.8 ± 13.4 years).

Methods—A 30° retinal field centered at the fovea was investigated using FLIO. This camera is based on a Heidelberg Engineering Spectralis system. Fundus autofluorescence (FAF) decays were detected in short (498–560 nm, SSC) and long (560–720 nm, LSC) spectral channels. The mean fluorescence lifetime, τ_m , was calculated from a 3-exponential approximation of the FAF decays. For MacTel patients, macular pigment (MP), OCT, blue light reflectance, fluorescein angiography, as well as fundus photography, were also recorded.

Main Outcome Measures—Mean FAF lifetime (τ_m) images.

Results—FLIO of MacTel patients shows a unique pattern of prolonged τ_m at the temporal side of the fovea in patients with MacTel in the “MacTel area” within $5\text{--}6^\circ$ of the foveal center. In early stages, this region appears crescent-shaped, while advanced stages show a ring-like pattern. This pattern corresponds well with other imaging modalities and gives an especially high contrast of the affected region even in minimally affected individuals. Additionally, FLIO provides a novel means to monitor the abnormal MP distribution. In one case, FLIO showed changes suggestive of MacTel within a clinically normal parent of two MacTel patients.

Conclusions—FLIO detects retinal changes in patients with MacTel with high contrast, presenting a distinctive signature that is a characteristic finding of the disease. The non-invasive

³Corresponding author: Paul S. Bernstein, John A. Moran Eye Center, University of Utah, 65 Mario Capecchi Drive, Salt Lake City, UT 84132, USA, Telephone: 801-581-6078, Fax: 801-581-3357, paul.bernstein@hsc.utah.edu.

Address for reprints: John A. Moran Eye Center, University of Utah, 65 Mario Capecchi Drive, Salt Lake City, UT 84132, USA

Meeting Presentation: Lowy Medical Research Institute (LMRI) Annual Meeting, 5/3 – 5/5 2017, New York City, USA, Deutsche Ophthalmologische Gesellschaft (DOG) Annual Meeting, 9/28 – 10/1 2017, Berlin, Germany

Conflict of Interest: No conflicting relationship exists for any author.

properties of this novel imaging modality provide a valuable addition to clinical assessment of early changes in the disease that could lead to more accurate diagnosis of MacTel.

Macular telangiectasia type 2 (MacTel) is an uncommon hereditary disease gradually resulting in vascular and neuro-degenerative changes, leading to metamorphopsia and central vision loss¹. Whereas macular telangiectasia type 1 is very rare and manifests typically as a unilateral disease in young males, type 2 is a bilateral disease with a later onset at 40 to 60 years²⁻⁴. Patients affected with MacTel show low scores on National Eye Institute Visual Function Questionnaires⁵. A prevalence of 0.06 to 0.1% has been reported; however, it is believed that this number is underestimated⁶. Due to the difficulty of early diagnosis, patients may be misdiagnosed with age-related macular degeneration (AMD) instead⁷. The pathogenesis behind the disease is still unknown; however, a dominant genetic inheritance with reduced penetrance is likely⁸⁻¹⁰. Although recently two genetic loci within the glycine/serine pathway were identified for MacTel, the actual genes related to the disease have not yet been found, and thus genetic testing is not yet available^{8, 11, 12}. It has been reported that a loss of Müller and photoreceptor cells plays a key role in the development of the disease^{13, 14}. The loss of the ellipsoid zone typically starts temporal to the foveal center and progresses in all directions and may eventually involve the entire MacTel area. It is associated with a loss of retinal sensitivity and eventual loss of visual acuity once the degeneration reaches the foveal center^{17, 18}. Additionally, an abnormal distribution of macular pigment (MP) at 5 to 9 degree eccentricity has been described¹⁹⁻²³. MP levels are generally low, yet may appear normal in early stages of the disease²⁴. Although changes in MP binding proteins do not appear to be associated with a loss of Müller cells, supplementation with carotenoids does not re-establish the typical MP distribution but rather causes a ring-like enhancement of MP outside of the fovea^{21, 25, 26}. Other findings in MacTel include intraretinal crystals in approximately 46% of patients, which typically appear at the level of the inner limiting membrane at all stages of the disease. The origin of these crystals remains unclear²⁷⁻³⁰.

Presently, there are no treatments for MacTel. Intravitreal steroid or anti-vascular endothelial growth factor injections have not been promising and seem to have no effect on improving visual outcome³¹⁻³³. The effect of ciliary neurotrophic factor may be beneficial and is currently under investigation^{34, 35}.

Multiple imaging modalities show unique changes within MacTel, including color fundus imaging, fundus autofluorescence (FAF) intensity imaging, optical coherence tomography (OCT), fluorescein angiography as well as blue-light reflectance imaging⁴¹⁻⁴⁴. Fluorescein angiography has historically been used as gold-standard imaging for MacTel; however, recently other non-invasive imaging modalities were proposed to be useful^{30, 41, 45-47}. Patients can be diagnosed when retinal damage is visible, but diagnosis at early stages is still challenging. At this point, there is no clear characteristic set of findings in the early course of MacTel, leading in many cases to delayed diagnosis. A lack of the foveal reflex and retinal graying are often the first clinical signs. Mildly ectatic capillaries in the deeper capillary network and dilated venules may develop later in the course of the disease. Retinal pigment clumps and foveal atrophy are often found in late stages of the disease³⁰. Retinal alterations often start at the temporal para-central side of the fovea³⁶. They may eventually

affect the entire so-called MacTel area, which has been described as an oval region with approximately 5° vertical and 6° horizontal eccentricities. This is the maximal area that is clinically affected in eyes with advanced MacTel^{37–39}. Increased central autofluorescence may be associated with poorer central visual acuity⁴⁰.

Fluorescence lifetime imaging ophthalmoscopy (FLIO) is new imaging technology that offers a novel approach for early diagnosis of various retinal diseases. FLIO reproducibly provides additional information on the autofluorescence of the retina^{48, 49}. Detecting FAF lifetimes enables the detection of subtle changes within retinal molecules at early stages of diseases. Molecule changes alter the FAF lifetimes, leading to different patterns within the retina^{48, 50–56}. These molecular changes may be an early predictor of retinal changes even before retinal damage is visible to an ophthalmologist. Additionally, FLIO depicts changes in MP in the course of various diseases, such as macular holes^{57, 58}. The high contrast with which FLIO highlights changes in the retina could lead to improved clinical detection of MacTel. This study investigates the potential benefit of FLIO imaging in patients with MacTel.

METHODS

Subjects

This prospective, cross-sectional study was Institutional Review Board approved and adhered to the Declaration of Helsinki. The study is HIPAA compliant. Informed written consent was obtained from the patients prior to all investigations.

All patients and healthy controls were examined between March and May 2017 and recruited from the Moran Eye Center.

Procedure

An ophthalmologist examined and diagnosed all patients with macular telangiectasia type 2 with confirmation by the Moorfields Eye Hospital Reading Centre. OCT, blue-light reflectance, fluorescein angiography and dual wavelength autofluorescence images were made available to the reading center. The central best corrected visual acuity (BCVA) was obtained. The intra-ocular pressure was measured with a Tono-Pen, and pupils were dilated.

After 30 minutes, a non-invasive FLIO measurement was performed with an acquisition time of approximately 2 minutes per eye. Additionally, a frequency domain OCT image as well as MP levels were obtained. MP was measured using dual wavelength autofluorescence imaging. Fundus photography, blue light reflectance, and fluorescein angiography were recorded as well.

FLIO-setup and Image Acquisition

Based on existing Heidelberg Engineering Spectralis technology, FLIO records FAF lifetimes from a 30° retinal field *in vivo* relying on the principle of time-correlated single photon counting^{59, 60}. The detailed setup and safety of FLIO have been described previously^{49, 57, 59}. Briefly, FAF is excited by a pulsed diode laser (473 nm, 80 MHz). Two hybrid photo-multipliers (HPM-100-40, Becker & Hickl GMBH, Berlin, Germany) detect

fluorescence photons, resulting in two separate spectral channels: the short spectral channel (SSC; 498 to 560 nm) and the long spectral channel (LSC; 560 to 720 nm). A high-contrast confocal infrared reflectance image for eye tracking is included. A photon arrival histogram, representing the probability density function of the decay process, is based on the detection of photons into 1024 time channels. To ensure reliable image quality, at least 1000 photons were recorded for each pixel as a minimal signal threshold.

The fluorescence data were analyzed using the Software SPCImage 4.4.2 (Becker & Hickl GmbH, Berlin, Germany). By calculating the least-square fit of a series of three exponential functions, the fluorescence decay was approximated. A 3×3 pixel binning was used for the purpose of noise reduction. The amplitude-weighted mean fluorescence decay time, τ_m , was used for further analysis, representing the amplitude-weighted average of the three time constants from the fit. Further details have been described elsewhere^{57, 60}

FLIMX was used for all FAF lifetime analyses and to generate pseudo-color images of the FAF lifetimes⁶¹. This software is documented and freely available for download online under the open source BSD-license (<http://www.flimx.de>). A standardized ETDRS grid was applied to obtain mean FAF lifetimes from different regions of interest (ROI): C (central fovea), T1 (inner temporal region), N1 (inner nasal region) and T2 (outer temporal region).

ImageJ was used to show the three-dimensional distribution of MP measured with the two-wavelength AF method.

Statistical Analysis

For all statistical analyses, SPSS 21 (SPSS Inc., Chicago, IL, USA) was employed. To test for significant τ_m differences between regions in one eye, a t-test for paired samples was used. To test for significant τ_m differences between subgroups (intraocular lens (IOL) versus natural lens, MacTel versus healthy individuals), we used an independent t-test. Data were checked for normal distribution.

RESULTS

Subjects

42 eyes of 21 patients with MacTel (mean age 60.5 ± 13.3) as well as 42 eyes of 25 healthy subjects (mean age 60.8 ± 13.4) were included in this study. Further details about the investigated groups can be found in Table 1.

Since the Moorfields Eye Hospital Reading Centre does not provide staging classification of MacTel eyes, we used our own system to divide MacTel eyes into four different stages according to fluorescein angiography leakage, non-invasive imaging, fundus examination, and visual acuity: “Early” refers to absent to slight temporal leakage with other imaging studies suggestive of MacTel (OCT, dual wavelength AF, blue light reflectance) and an otherwise healthy fundus examination. “Intermediate” refers to more prominent temporal leakage typically with changes in visual acuity (VA 20/30 or worse) and/or obvious pigmentary changes. “Advanced” includes eyes with strong leakage in the entire MacTel region or a history of choroidal neovascularization, and “Atrophy” refers to atrophic changes

within the MacTel region; this was found in seven eyes. These “Atrophy” cases were not included in statistical analysis, leaving 36 eyes for statistical investigation.

Five of the investigated MacTel eyes and six of the healthy control eyes were pseudophakic. No significant difference in the four investigated ROI between controls with IOLs and eyes with a natural lens was found (p-value ranging from 0.10 to 0.14). In the foveal ROI (area C) of MacTel eyes, no significant difference was found between IOL eyes and eyes with a natural lens (p = 0.66). However, the other three regions showed significant differences (p<0.05) between those groups. Eyes with IOLs showed about 90 ± 40 ps shorter FAF lifetimes than eyes with natural lenses for any of those regions. All IOL eyes in the MacTel patients had advanced MacTel.

Two patients reported long-term supplementation (> one year) of 10 mg zeaxanthin per day, and five other patients reported taking the AREDS 2 formula for over one year (10 mg lutein + 2 mg zeaxanthin per day).

FLIO and Other Retinal Imaging in MacTel

Eyes affected with MacTel showed a significantly changed pattern of FAF lifetimes as compared to healthy control eyes. Figure 1 shows the FAF intensity and lifetime images of a healthy eye and a typical eye with early-stage MacTel. We found a prolongation of τ_m within the so-called MacTel area, manifested as a blue color-coded signal temporally parafoveal, visible in both spectral channels. For simplification we focused on the SSC because here the parafoveal MacTel FLIO changes were more pronounced, and the MP (orange spot at the fovea in normal eyes) better visualized.

In eyes with early and intermediate stages of MacTel, we observed a crescent-shaped prolongation of τ_m at the temporal side of the fovea. In advanced stages, the prolongation of τ_m appeared to be wrapped around the fovea in a ring-like pattern. The prolongation may then also affect the foveal and the nasal region. In seven subjects with very advanced stages of the disease, we found atrophic changes within the MacTel area. The FAF lifetimes in atrophic lesions did not follow a crescent shape pattern anymore; they rather affected the entire oval-shaped MacTel area.

We compared FAF lifetimes over different regions of interest from a standardized ETDRS grid (Figure 2 (C)). Mean FAF lifetimes of eyes with different stages of MacTel (excluding eyes with atrophic lesions) as well as age-matched healthy controls were analyzed and compared. In detail, the region T1 was compared to the regions T2, C and N1. Healthy eyes exhibited the typical and previously described pattern with shortest FAF lifetimes in the macular region and medium-long τ_m in all other regions. In healthy eyes, τ_m in T1 was significantly shorter than in N1 (p<0.001) and C (p<0.001). τ_m in T1 was slightly but not significantly shorter than in T2. Eyes affected with MacTel showed longest FAF lifetimes within T1, which were significantly longer than all other regions (p<0.001). In a separate analysis that was performed on only those eyes with early MacTel, the prolongation of T1 was even more apparent. Table 2 shows the FAF lifetimes.

Comparing ROI over MacTel eyes to healthy eyes, significant differences were found within the regions of the MacTel area (C, N1, T1; $p < 0.001$), but no significant difference was found between these groups in region T2 ($p=0.17$).

Comparing only “Early” MacTel eyes to the group of healthy eyes, significant differences were found for T1 and C ($p < 0.001$), yet not for N1 or T2. Area C was approximately 88 ± 25 ps longer, and area T1 was 110 ± 26 ps longer for patients with MacTel.

Looking at relative differences, T1 minus T2 was -3 ± 20 ps for healthy eyes, whereas the same difference was 63 ± 40 ps for eyes with MacTel. This means that in healthy eyes, T1 was approximately 3 ps shorter than T2 whereas in MacTel eyes, T1 was about 63 ps longer than T2. The difference between healthy and MacTel eyes was 65 ± 7 ps, $p < 0.001$ (Figure 2 (D)). The relative ratio between these two regions (T2/T1) was 1.02 ± 0.08 in the controls, whereas it was 0.84 ± 0.09 in eyes affected with MacTel. In MacTel eyes, the ratio ranged from 0.63 to 0.97, healthy eyes ranged from 0.90 to 1.30. The mean difference in T2/T1 ratios between healthy and MacTel eyes was 0.20 ± 0.02 , $p < 0.001$ (Figure 2 (E)).

Figure 3 shows the MacTel area in different imaging modalities: FAF lifetime and intensity imaging, fluorescein angiography, blue light reflectance, fundus photography and OCT. One eye of each stage (early, intermediate, and advanced) of MacTel is presented. The affected region clearly stands out with high contrast in the FLIO images, showing the prolonged τ_m in blue color.

Macular Pigment in MacTel

MP showed an abnormal distribution in many eyes with MacTel. In general, patients not taking carotenoid supplementation demonstrated low levels of MP in the present study. The MP often formed a ring-like pattern at 5 to 9 degrees outside of the fovea. A central peak was still found in some patients with early to intermediate MacTel. Yet even with long-term supplementation of lutein and zeaxanthin, not every patient showed a central peak of MP. Figure 4 depicts our findings regarding MP. Patient A received zeaxanthin (10 mg/day) for over five years, whereas patient B never took any supplementation. The overall levels of MP were higher for patient A (13194 a.u.) as compared to patient B (2883 a.u.). This is reflected within the FAF lifetimes, which were shorter for patient A. The distribution of MP is also reflected in short FAF lifetimes.

Crystals in MacTel

Ten MacTel eyes showed evidence of crystals on clinical examination and in fundus photography. From an overlay of fundus photos with FAF lifetime images, it is clearly visible that crystals were found within the region of prolonged τ_m and not within areas of MP (Figure 5). Different overlays were used to try to identify the exact location of crystals. Furthermore, the clinically used FAF intensity imaging, recording broad emission from 500 to 700 nm, did not show these crystals, while the SSC FAF intensity image (498 – 560 nm) showed hyperfluorescence at the spots of the crystals.

Family Analysis

In our experience, MacTel can often be diagnosed in at least one parent of affected patients. However, in one family, both living parents of two MacTel subjects had completely normal clinical examinations and complete imaging studies. The Moorfields Eye Hospital Reading Centre and the clinician graded both as “unaffected”. Nevertheless, when conducting FLIO, the mother of these siblings showed T2/T1 ratios of 0.93 and 0.95, whereas the father showed ratios of 0.98 and 0.99. This suggests that the mother is more likely to carry the putative gene for MacTel. Additionally, not only was the ratio slightly lower for the mother, she also presents a prolongation of FAF lifetimes in the superior area of the MacTel area that was not seen in the father. When we examined two sisters of the mother, very similar FLIO changes were found in one of them. Figure 6 shows the findings of FLIO of the patient and her parents.

DISCUSSION

The diagnosis of MacTel is currently based on clinical findings and retinal imaging. Whereas advanced stages of the disease have common imaging characteristics, early diagnosis is often challenging, and many different imaging modalities may provide incomplete information^{41–44}. As the search for gene(s) underlying MacTel continues, and clinical trials concerning neuroprotection are promising and currently under clinical investigation, the need for a reliable diagnostic modality is rising³⁴. This may be especially necessary for early or slight changes within the retina in familial studies, ideally before cells have been damaged, and for longitudinal follow up in therapeutic trials. Our study shows a novel imaging modality called fluorescence lifetime imaging ophthalmoscopy (FLIO), that is able to consistently and quantitatively detect even small changes in the fundus of MacTel patients.

FLIO is designed to monitor changes within the human retina *in vivo*. Typical patterns have been previously described for healthy eyes^{48, 49, 57}. A variety of different retinal conditions, such as diabetic retinopathy, AMD, Alzheimer’s disease, choroideremia, central serous chorioretinopathy, Stargardt disease, and retinal artery occlusion have also been investigated using FLIO^{52–56, 62–64}. Additionally, studies on healthy subjects and patients with macular holes have demonstrated the influence of MP in FLIO^{57, 58}. This may be beneficial for early diagnosis as MP seems to be involved in the early changes within MacTel.

FLIO shows specific changes in MacTel, which are unlike any other FLIO patterns previously described for other eye diseases. Representative examples of these changes are presented in Figures 1 and 3. While FLIO highlighted changes in MP such as low foveal concentrations and ring-shaped patterns, we also observed a significant prolongation of τ_m at the temporal side of the fovea in early stages and in the entire MacTel area in advanced stages. FLIO gave a high contrast image of the affected MacTel area amenable to quantitative analysis, which in many cases seemed more readily apparent relative to other commonly used MacTel imaging modalities such as OCT, dual wavelength autofluorescence, and blue light reflectance. The non-invasive and relatively quick measurement (two minutes) has advantages over other imaging modalities such as fluorescein angiography. As compared to an age-matched group of healthy individuals, the

typical MacTel region temporal to the fovea (T1) in the “Early” stage presented itself as significantly prolonged by approximately 110 ± 26 ps. A distant adjacent temporal region (T2), located outside of the MacTel area, served as a convenient reference region, as there was no significant difference between healthy and MacTel eyes in this region. τ_m in T1 was significantly longer than T2 in MacTel patients, but about the same or even slightly shorter in normal subjects.

Relative differences revealed similar changes. Whereas T1 was approximately 3 ps shorter than T2 in healthy eyes, T1 was about 63 ps longer than T2 in eyes affected with MacTel. This difference may be an indicator of the disease. Furthermore, relative ratios between these two regions (T2/T1) showed that a ratio above 1.0 is likely to be healthy, whereas a ratio below 0.9 (in combination with typical FLIO features) is likely to be affected with MacTel. The ratio 0.9 to 1.0 is borderline, so further investigation of FAF lifetime image patterns might be helpful in these cases.

MP often enhances in a ring around the MacTel area. Why this pattern occurs in MacTel is still unknown²⁵. The MacTel area typically has an ellipsoid shape, but the circularly averaged presentation of the MP distribution produced by the Spectralis software does not demonstrate it well in MacTel patients, as shown in Figure 4. With some additional effort and re-analysis with ImageJ, the anomalous MP distribution can be presented in a three-dimensional way. FLIO may present an alternative way to show the MP distribution in MacTel. We can also monitor changes within MacTel and the effect of supplementation (foveal versus ring-like enhancement).

Another important finding of the present study was the persistent presence of MP in the center of the fovea in early stages of MacTel. From our observations, the most vulnerable spot appeared to be the temporal side of the fovea. We can speculate from these findings that there may be nasal-temporal variability in vascular supply, leading to an accumulation of different molecules in these regions. This theory is supported by the topographical distribution of crystals, which, when found in our patients, always occurred within the area of prolonged τ_m .

In terms of the significance of crystals in MacTel, we can only observe that crystals present themselves in OCT-images within the inner limiting membrane. At the current time, it remains to be determined whether they are caused by oxidative, neuro-degenerative, or perhaps other effects. The composition of the crystals remains unclear, as does the reason why they may form²⁷. The lateral resolution of FLIO is approximately $10 \mu\text{m}$, whereas crystals were described as $5 \mu\text{m}$ or larger²⁷. Whether the crystals are responsible for a hyperfluorescence found in these spots in the SSC needs to be evaluated further in *ex vivo* studies. Nevertheless, as shown in Figure 5, they were never found in the area of MP, and unlike MP, they did not show black color in conventional FAF intensity images. Therefore, we can exclude MP as the source of crystals within MacTel. Whether Müller cells, which supposedly play a role in the early course of the disease, are involved in the formation of crystals needs to be further evaluated^{13, 14}.

We investigated one pair of parents with two affected children. Assuming an autosomal dominant inheritance, at least one of the parents must be a carrier of a putative MacTel gene⁸⁻¹⁰. Comparing both parents, the mother presented a FLIO pattern that makes her more likely to be the carrier of a putative MacTel gene. The mother's relative ratio of T2/T1 was lower than the father's, and she exhibited prolongation of FAF lifetimes in the superior area of the MacTel area. Although we cannot give the mother the diagnosis of MacTel based solely on these FLIO changes because the T2/T1 ratios of the mother and the father are in the grey zone, when one looks at both the qualitative and quantitative data, the mother is more likely to be affected. Further family investigations showed that one of the mother's two sisters also showed similar findings. Neither the mother nor her sister had any visual complaints, and their fundus examinations and other imaging studies were normal.

This suggests that FLIO may be very sensitive for changes in MacTel. FLIO may go beyond other imaging modalities, showing changes within the retina even before there is any leakage in fluorescein angiography or abnormalities in other imaging methods. FLIO may prove invaluable for detecting subclinical cases of MacTel in younger members of MacTel families with no other signs or symptoms, greatly facilitating causative gene identification in this late-onset macular disease with apparent autosomal dominant inheritance and reduced penetrance. This needs to be further investigated on additional first-degree family members and longitudinal follow-up studies.

A strength of this study lies in the fact that we could image more than 20 well characterized individuals with what has been considered to be a relatively rare retinal disease⁷. Nevertheless, a larger number of eyes may reveal additional information on the manifestations of the disease. This study is a cross-sectional study and gives no information on the progression of MacTel, so longitudinal follow-up studies are indicated, especially for the eyes which showed changes in FLIO only. We utilized a standardized ETDRS-grid to obtain reproducible mean FAF lifetimes from different ROI. Smaller grids in a more crescent-shaped form may describe the changes within the MacTel area more accurately. Nevertheless, the ETDRS grid showed highly significant differences within these regions.

Another limitation lies within the effect of IOLs. Five eyes of three MacTel patients had IOLs. Eyes with IOLs showed the same FLIO patterns as eyes with natural lenses. For comparison we included six healthy subjects with IOLs, where no difference in τ_m was found between IOLs and natural lenses in healthy eyes. All MacTel patients with IOLs had "Advanced" MacTel. In this group, other patients showed cataracts, which enlarges the differences in τ_m . The fovea of four out of five IOL patients with MacTel was largely affected (prolongation of τ_m ; three outliers in Figure 2 (B) from IOL patients); here retinal changes again have a stronger impact on retinal τ_m than the lens. We believe that a larger number of IOL eyes including IOL patients with early MacTel would result in no significant differences regarding the lens status.

We did not exclude patients with MacTel and additional other retinal diseases, such as AMD and a history of macular hole, or vitreal floaters. These conditions were monitored but they cannot account for the typical MacTel FLIO pattern. Nevertheless, advanced retinal diseases may in other cases disturb the typical pattern found in eyes with MacTel.

In conclusion, FLIO shows a specific pattern in MacTel with a crescent-shaped prolongation of τ_m towards the temporal side of the fovea. This pattern is in accordance with other clinical findings and often correlates with leakage in fluorescein angiography; however, FLIO goes beyond this in some cases, especially in early stages of MacTel. An eye with a ratio of T2/T1 <0.9 in combination with typical FLIO features is likely to be affected with MacTel. FLIO is able to show typical MacTel changes even without fluorescein angiographic leakage. Furthermore, FLIO is non-invasive and therefore easy to conduct in the clinical setting. Finally, we also obtain information on the nutrition status and the MP distribution within the retina, which may be very helpful as MP changes may occur early in the disease. Further longitudinal studies are necessary to obtain information if FLIO can predict early development of MacTel.

Acknowledgments

The authors gratefully thank Heidelberg Engineering for providing the FLIO as well as for their technical assistance. We would like to thank Matthias Klemm for providing the FLIMX software. The authors also thank the Lowy Medical Research Institute (LMRI) for their support. Additional support was provided by NIH grants EY11600 and EY14800 and Research to Prevent Blindness.

ABBREVIATIONS

AMD	Age-related macular degeneration
FAF	Fundus autofluorescence
FLIO	Fluorescence lifetime imaging ophthalmoscopy
IOL	Intraocular lens
LSC	Long spectral channel
OCT	Optical coherence tomography
MacTel	Macular telangiectasia type 2
MP	Macular pigment
ROI	Region(s) of interest
SSC	Short spectral channel

References

1. Charbel Issa P, Holz FG, Scholl HP. Metamorphopsia in patients with macular telangiectasia type 2. *Doc Ophthalmol.* 2009; 119(2):133–40. [PubMed: 19711108]
2. Charbel Issa P, Gillies MC, Chew EY, et al. Macular telangiectasia type 2. *Prog Retin Eye Res.* 2013; 34:49–77. [PubMed: 23219692]
3. Clemons TE, Gillies MC, Chew EY, et al. Baseline characteristics of participants in the natural history study of macular telangiectasia (MacTel) MacTel Project Report No. 2. *Ophthalmic Epidemiol.* 2010; 17(1):66–73. [PubMed: 20100102]
4. Finger RP, Charbel Issa P, Fimmers R, et al. Reading performance is reduced by parafoveal scotomas in patients with macular telangiectasia type 2. *Invest Ophthalmol Vis Sci.* 2009; 50(3): 1366–70. [PubMed: 18997085]

5. Clemons TE, Gillies MC, Chew EY, et al. The National Eye Institute Visual Function Questionnaire in the Macular Telangiectasia (MacTel) Project. *Invest Ophthalmol Vis Sci.* 2008; 49(10):4340–6. [PubMed: 18586874]
6. Sallo FB, Leung I, Mathenge W, et al. The prevalence of type 2 idiopathic macular telangiectasia in two African populations. *Ophthalmic Epidemiol.* 2012; 19(4):185–9. [PubMed: 22364548]
7. Klein R, Blodi BA, Meuer SM, et al. The prevalence of macular telangiectasia type 2 in the Beaver Dam eye study. *Am J Ophthalmol.* 2010; 150(1):55–62. e2. [PubMed: 20609708]
8. Parmalee NL, Schubert C, Figueroa M, et al. Identification of a potential susceptibility locus for macular telangiectasia type 2. *PLoS One.* 2012; 7(8):e24268. [PubMed: 22952568]
9. Gillies MC, Zhu M, Chew E, et al. Familial asymptomatic macular telangiectasia type 2. *Ophthalmology.* 2009; 116(12):2422–9. [PubMed: 19815294]
10. Delaere L, Spielberg L, Leys AM. Vertical transmission of macular telangiectasia type 2. *Retin Cases Brief Rep.* 2012; 6(3):253–7. [PubMed: 25389724]
11. Parmalee NL, Schubert C, Merriam JE, et al. Analysis of candidate genes for macular telangiectasia type 2. *Mol Vis.* 2010; 16:2718–26. [PubMed: 21179236]
12. Scerri TS, Quagliari A, Cai C, et al. Genome-wide analyses identify common variants associated with macular telangiectasia type 2. *Nat Genet.* 2017; 49(4):559–67. [PubMed: 28250457]
13. Powner MB, Gillies MC, Tretiach M, et al. Perifoveal muller cell depletion in a case of macular telangiectasia type 2. *Ophthalmology.* 2010; 117(12):2407–16. [PubMed: 20678804]
14. Powner MB, Gillies MC, Zhu M, et al. Loss of Muller's cells and photoreceptors in macular telangiectasia type 2. *Ophthalmology.* 2013; 120(11):2344–52. [PubMed: 23769334]
15. Heeren TF, Clemons T, Scholl HP, et al. Progression of Vision Loss in Macular Telangiectasia Type 2. *Invest Ophthalmol Vis Sci.* 2015; 56(6):3905–12. [PubMed: 26070062]
16. Schmitz-Valckenberg S, Ong EE, Rubin GS, et al. Structural and functional changes over time in MacTel patients. *Retina.* 2009; 29(9):1314–20. [PubMed: 19491718]
17. Peto T, Heeren TFC, Clemons TE, et al. CORRELATION OF CLINICAL AND STRUCTURAL PROGRESSION WITH VISUAL ACUITY LOSS IN MACULAR TELANGIECTASIA TYPE 2: MacTel Project Report No. 6-The MacTel Research Group. *Retina.* 2017
18. Sallo FB, Peto T, Egan C, et al. The IS/OS junction layer in the natural history of type 2 idiopathic macular telangiectasia. *Invest Ophthalmol Vis Sci.* 2012; 53(12):7889–95. [PubMed: 23092925]
19. Helb HM, Charbel Issa P, RL VDV, et al. Abnormal macular pigment distribution in type 2 idiopathic macular telangiectasia. *Retina.* 2008; 28(6):808–16. [PubMed: 18536596]
20. Delori FC, Goger DG, Hammond BR, et al. Macular pigment density measured by autofluorescence spectrometry: comparison with reflectometry and heterochromatic flicker photometry. *J Opt Soc Am A Opt Image Sci Vis.* 2001; 18(6):1212–30. [PubMed: 11393613]
21. Zeimer MB, Padge B, Heimes B, Pauleikhoff D. Idiopathic macular telangiectasia type 2: distribution of macular pigment and functional investigations. *Retina.* 2010; 30(4):586–95. [PubMed: 20386096]
22. Degli Esposti S, Egan C, Bunce C, et al. Macular pigment parameters in patients with macular telangiectasia (MacTel) and normal subjects: implications of a novel analysis. *Invest Ophthalmol Vis Sci.* 2012; 53(10):6568–75. [PubMed: 22899764]
23. Bernstein PS, Li B, Vachali PP, et al. Lutein, zeaxanthin, and meso-zeaxanthin: The basic and clinical science underlying carotenoid-based nutritional interventions against ocular disease. *Prog Retin Eye Res.* 2016; 50:34–66. [PubMed: 26541886]
24. Chin EK, Kim DY, Hunter AA 3rd, et al. Staging of macular telangiectasia: power-Doppler optical coherence tomography and macular pigment optical density. *Invest Ophthalmol Vis Sci.* 2013; 54(7):4459–70. [PubMed: 23716628]
25. Choi RY, Gorusupudi A, Wegner K, et al. Macular Pigment Distribution Responses to High-Dose Zeaxanthin Supplementation in Patients with Macular Telangiectasia Type 2. *Retina.* 2017
26. Li B, Vachali PP, Shen Z, et al. Retinal accumulation of zeaxanthin, lutein, and beta-carotene in mice deficient in carotenoid cleavage enzymes. *Exp Eye Res.* 2017; 159:123–31. [PubMed: 28286282]

27. Sallo FB, Leung I, Chung M, et al. Retinal crystals in type 2 idiopathic macular telangiectasia. *Ophthalmology*. 2011; 118(12):2461–7. [PubMed: 21839520]
28. Ryu CL, Mikhail M, Khan A, et al. Macular Telangiectasia Type 2 in an Otherwise Healthy Teenage Boy with Consanguineous Parents. *Retin Cases Brief Rep*. 2016
29. Baumuller S, Charbel Issa P, Scholl HP, et al. Outer retinal hyperreflective spots on spectral-domain optical coherence tomography in macular telangiectasia type 2. *Ophthalmology*. 2010; 117(11):2162–8. [PubMed: 20557944]
30. Gass JD, Blodi BA. Idiopathic juxtafoveolar retinal telangiectasis. Update of classification and follow-up study. *Ophthalmology*. 1993; 100(10):1536–46. [PubMed: 8414413]
31. Mehta H, Muller S, Egan CA, et al. Natural history and effect of therapeutic interventions on subretinal fluid causing foveal detachment in macular telangiectasia type 2. *Br J Ophthalmol*. 2016
32. Kovach JL, Rosenfeld PJ. Bevacizumab (avastin) therapy for idiopathic macular telangiectasia type II. *Retina*. 2009; 29(1):27–32. [PubMed: 18936721]
33. Roller AB, Folk JC, Patel NM, et al. Intravitreal bevacizumab for treatment of proliferative and nonproliferative type 2 idiopathic macular telangiectasia. *Retina*. 2011; 31(9):1848–55. [PubMed: 21610563]
34. Chew EY, Clemons TE, Peto T, et al. Ciliary neurotrophic factor for macular telangiectasia type 2: results from a phase 1 safety trial. *Am J Ophthalmol*. 2015; 159(4):659–66. e1. [PubMed: 25528956]
35. Bucher F, Walz JM, Buhler A, et al. CNTF Attenuates Vasoproliferative Changes Through Upregulation of SOCS3 in a Mouse-Model of Oxygen-Induced Retinopathy. *Invest Ophthalmol Vis Sci*. 2016; 57(10):4017–26. [PubMed: 27494343]
36. Davidorf FH, Pressman MD, Chambers RB. Juxtafoveal telangiectasis—a name change? *Retina*. 2004; 24(3):474–8. [PubMed: 15187680]
37. Abujamra S, Bonanomi MT, Cresta FB, et al. Idiopathic juxtafoveolar retinal telangiectasis: clinical pattern in 19 cases. *Ophthalmologica*. 2000; 214(6):406–11. [PubMed: 11054001]
38. Barthelmes D, Sutter FK, Gillies MC. Differential optical densities of intraretinal spaces. *Invest Ophthalmol Vis Sci*. 2008; 49(8):3529–34. [PubMed: 18441298]
39. Charbel Issa P, Helb HM, Rohrschneider K, et al. Microperimetric assessment of patients with type 2 idiopathic macular telangiectasia. *Invest Ophthalmol Vis Sci*. 2007; 48(8):3788–95. [PubMed: 17652753]
40. Balaskas K, Leung I, Sallo FB, et al. Associations between autofluorescence abnormalities and visual acuity in idiopathic macular telangiectasia type 2: MacTel project report number 5. *Retina*. 2014; 34(8):1630–6. [PubMed: 24743635]
41. Wong WT, Forooghian F, Majumdar Z, et al. Fundus autofluorescence in type 2 idiopathic macular telangiectasia: correlation with optical coherence tomography and microperimetry. *Am J Ophthalmol*. 2009; 148(4):573–83. [PubMed: 19573860]
42. Niskopoulou M, Balaskas K, Leung I, et al. Is indocyanine green angiography useful for the diagnosis of macular telangiectasia type 2? *Br J Ophthalmol*. 2013; 97(7):946–8. [PubMed: 23532616]
43. Surguch V, Gamulescu MA, Gabel VP. Optical coherence tomography findings in idiopathic juxtafoveal retinal telangiectasis. *Graefes Arch Clin Exp Ophthalmol*. 2007; 245(6):783–8. [PubMed: 17120013]
44. Sallo FB, Peto T, Egan C, et al. "En face" OCT imaging of the IS/OS junction line in type 2 idiopathic macular telangiectasia. *Invest Ophthalmol Vis Sci*. 2012; 53(10):6145–52. [PubMed: 22899757]
45. Wu L, Evans T, Arevalo JF. Idiopathic macular telangiectasia type 2 (idiopathic juxtafoveolar retinal telangiectasis type 2A, Mac Tel 2). *Surv Ophthalmol*. 2013; 58(6):536–59. [PubMed: 24160729]
46. Sallo FB, Leung I, Clemons TE, et al. Multimodal imaging in type 2 idiopathic macular telangiectasia. *Retina*. 2015; 35(4):742–9. [PubMed: 25412037]
47. Toto L, Di Antonio L, Mastropasqua R, et al. Multimodal Imaging of Macular Telangiectasia Type 2: Focus on Vascular Changes Using Optical Coherence Tomography Angiography. *Invest Ophthalmol Vis Sci*. 2016 Oct; 57(9):268–76.

48. Klemm M, Dietzel A, Haueisen J, et al. Repeatability of autofluorescence lifetime imaging at the human fundus in healthy volunteers. *Curr Eye Res.* 2013; 38(7):793–801. [PubMed: 23530995]
49. Dysli C, Quellec G, Abegg M, et al. Quantitative analysis of fluorescence lifetime measurements of the macula using the fluorescence lifetime imaging ophthalmoscope in healthy subjects. *Invest Ophthalmol Vis Sci.* 2014; 55(4):2106–13. [PubMed: 24569585]
50. Schweitzer D. Metabolic Mapping. In: Holz F, Spaide R, editors *Medical Retina*. Springer Berlin Heidelberg; 2010.
51. Schweitzer D, Schenke S, Hammer M, et al. Towards metabolic mapping of the human retina. *Microsc Res Tech.* 2007; 70(5):410–9. [PubMed: 17393496]
52. Schweitzer D, Deutsch L, Klemm M, et al. Fluorescence lifetime imaging ophthalmoscopy in type 2 diabetic patients who have no signs of diabetic retinopathy. *J Biomed Opt.* 2015; 20(6):61106. [PubMed: 25769278]
53. Schmidt J, Peters S, Sauer L, et al. Fundus autofluorescence lifetimes are increased in non-proliferative diabetic retinopathy. *Acta Ophthalmol.* 2016
54. Jentsch S, Schweitzer D, Schmidtke KU, et al. Retinal fluorescence lifetime imaging ophthalmoscopy measures depend on the severity of Alzheimer's disease. *Acta Ophthalmol.* 2014
55. Dysli C, Wolf S, Hatz K, Zinkernagel MS. Fluorescence Lifetime Imaging in Stargardt Disease: Potential Marker for Disease Progression. *Invest Ophthalmol Vis Sci.* 2016; 57(3):832–41. [PubMed: 26934141]
56. Dysli C, Wolf S, Zinkernagel MS. Autofluorescence Lifetimes in Geographic Atrophy in Patients With Age-Related Macular Degeneration. *Invest Ophthalmol Vis Sci.* 2016; 57(6):2479–87. [PubMed: 27149697]
57. Sauer L, Schweitzer D, Ramm L, et al. Impact of Macular Pigment on Fundus Autofluorescence Lifetimes. *Invest Ophthalmol Vis Sci.* 2015; 56(8):4668–79. [PubMed: 26207302]
58. Sauer L, Peters S, Schmidt J, et al. Monitoring Macular Pigment changes in Macular Holes using Fluorescence Lifetime Imaging Ophthalmoscopy (FLIO). *Acta Ophthalmol (Copenh).* 2016
59. Schweitzer D, Hammer M, Schweitzer F, et al. In vivo measurement of time-resolved autofluorescence at the human fundus. *J Biomed Opt.* 2004; 9(6):1214–22. [PubMed: 15568942]
60. Becker W. *The bh TCSPC Handbook*. 6. Berlin: Becker & Hickl GmbH; 2014.
61. Klemm M, Schweitzer D, Peters S, et al. FLIMX: A Software Package to Determine and Analyze the Fluorescence Lifetime in Time-Resolved Fluorescence Data from the Human Eye. *PLoS One.* 2015; 10(7):e0131640. [PubMed: 26192624]
62. Dysli C, Berger L, Wolf S, Zinkernagel MS. Fundus Autofluorescence Lifetimes and Central Serous Chorioretinopathy. *Retina.* 2017
63. Dysli C, Wolf S, Tran HV, Zinkernagel MS. Autofluorescence Lifetimes in Patients With Choroideremia Identify Photoreceptors in Areas With Retinal Pigment Epithelium Atrophy. *Invest Ophthalmol Vis Sci.* 2016; 57(15):6714–21. [PubMed: 27951593]
64. Dysli C, Wolf S, Zinkernagel MS. Fluorescence lifetime imaging in retinal artery occlusion. *Invest Ophthalmol Vis Sci.* 2015; 56(5):3329–36. [PubMed: 26024116]

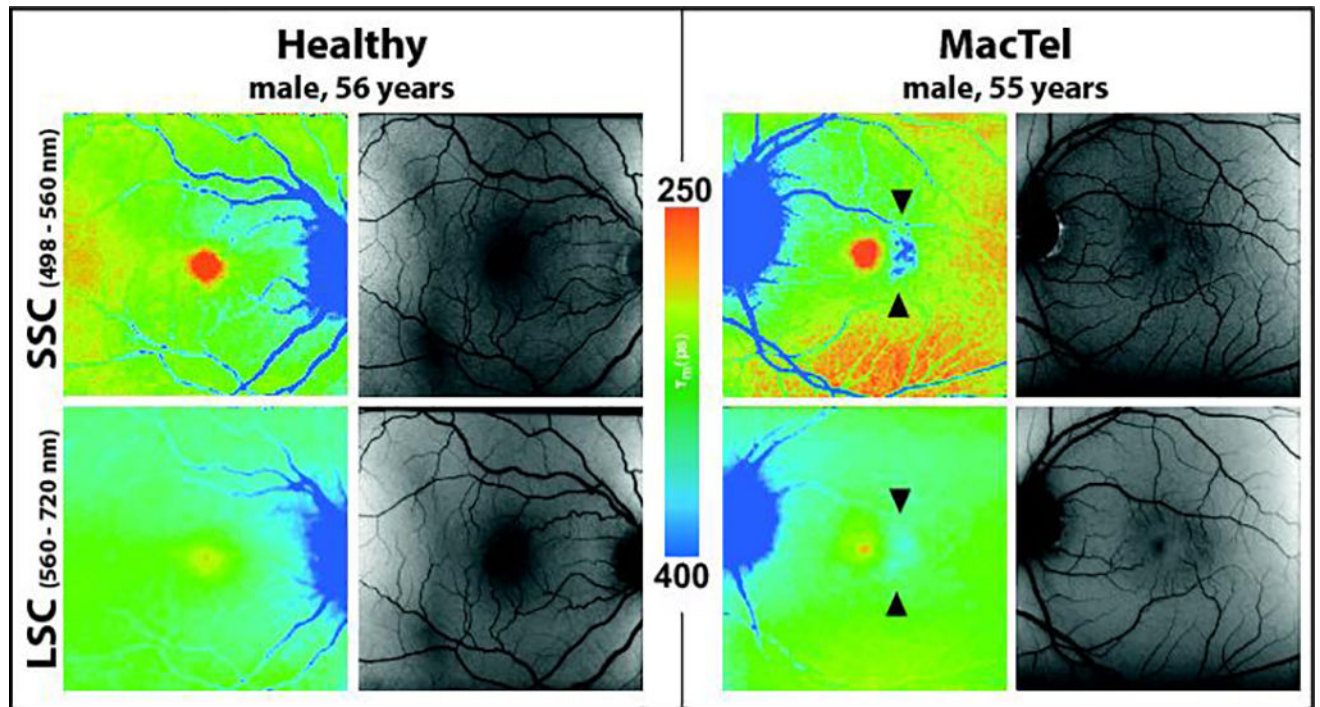


Figure 1. Typical FAF lifetime (color) and intensity (grey) images from the short spectral channel (SSC, 498 – 560 nm) and the long spectral channel (LSC, 560 – 720 nm) in a 56 year healthy individual as well as a 55 year old patient with early MacTel showing characteristic prolongation of FAF lifetimes (blue) temporal to the fovea in the MacTel area (see arrows).

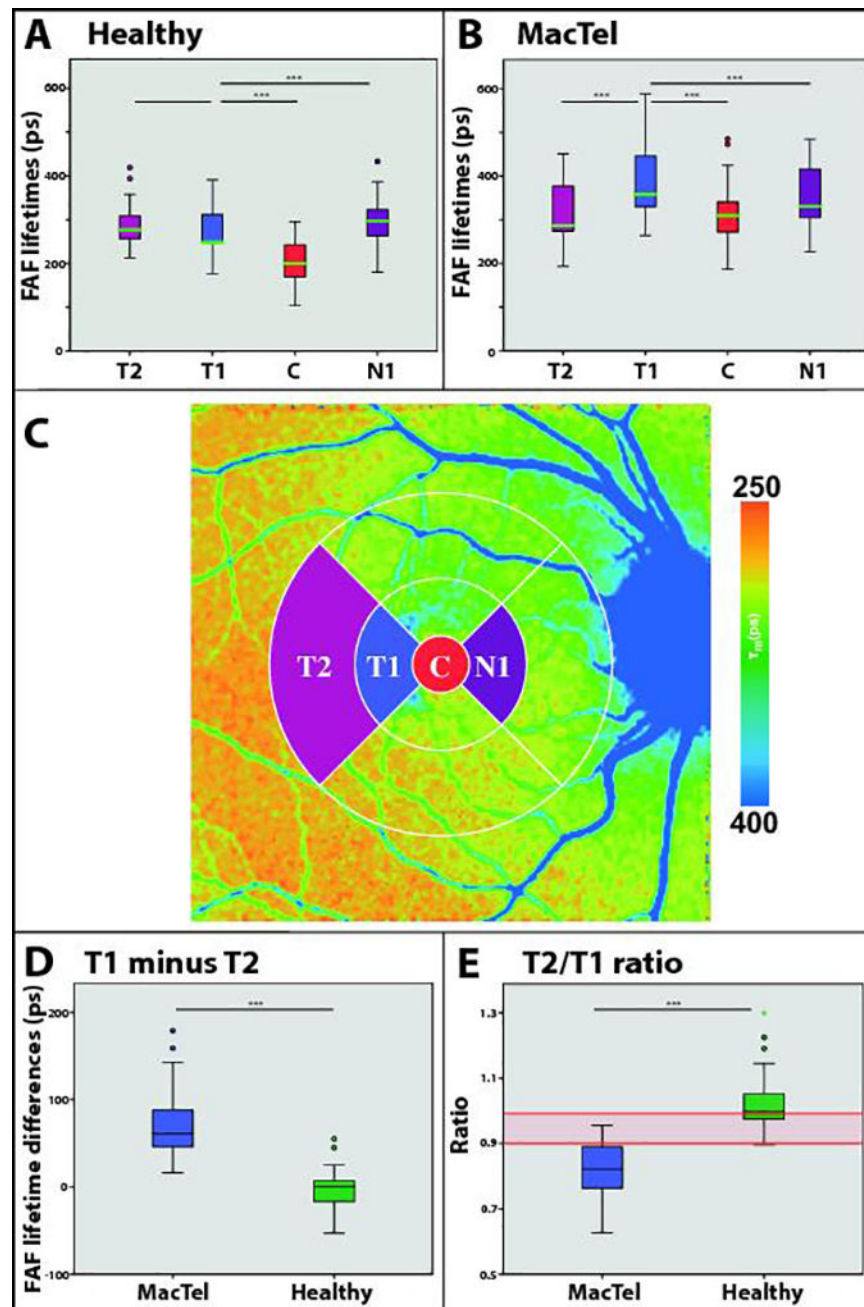


Figure 2. FAF lifetimes of different regions of interest (ROI) in healthy eyes (A) and MacTel (B). (***) indicates $p < 0.001$. (C) shows defined ROI. (D) shows FAF lifetime differences between T1 and T2 (T1 minus T2) between MacTel and healthy eyes. (E) gives the ratio of T2/T1. Red lines indicate defined cut-offs for healthy versus MacTel. $N=36$ for all.

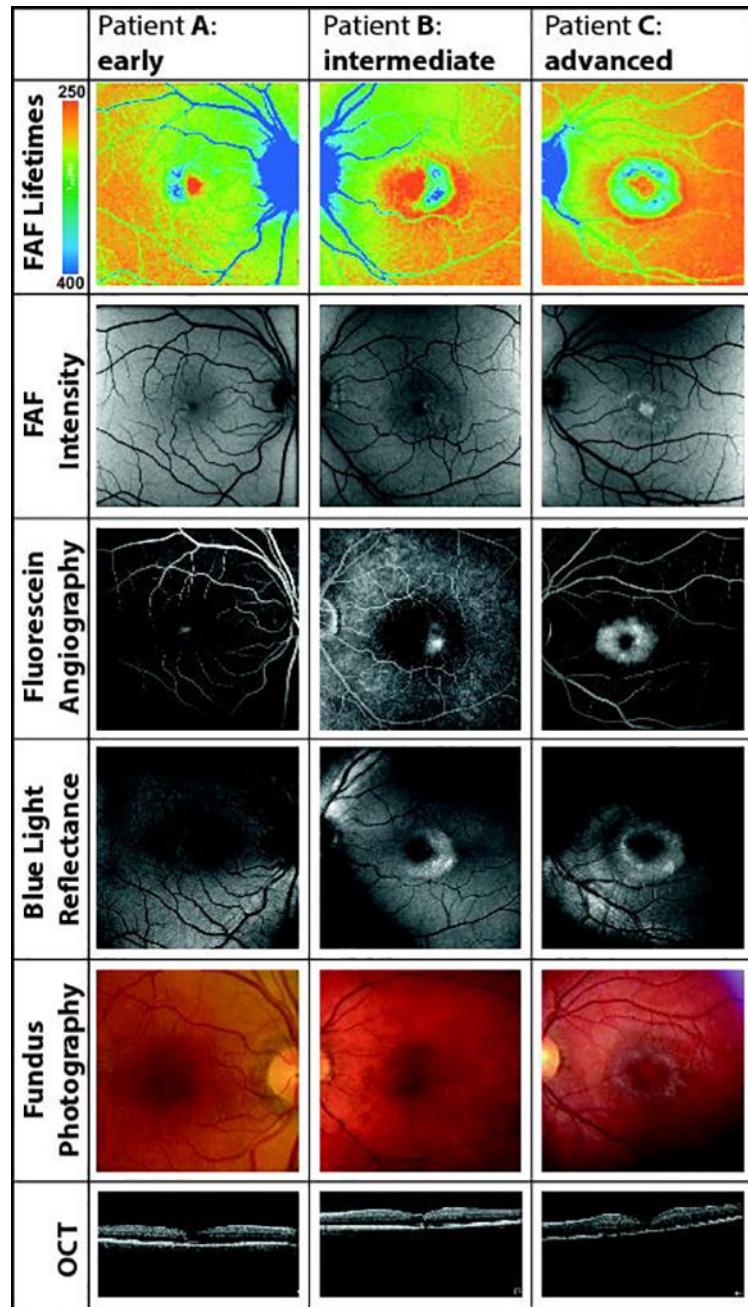


Figure 3. Visualization of the MacTel area from patient A with early, B with intermediate, and C with advanced MacTel. FAF lifetime and intensity images as well as fluorescein angiography, blue light reflectance, fundus photography and OCT are shown.

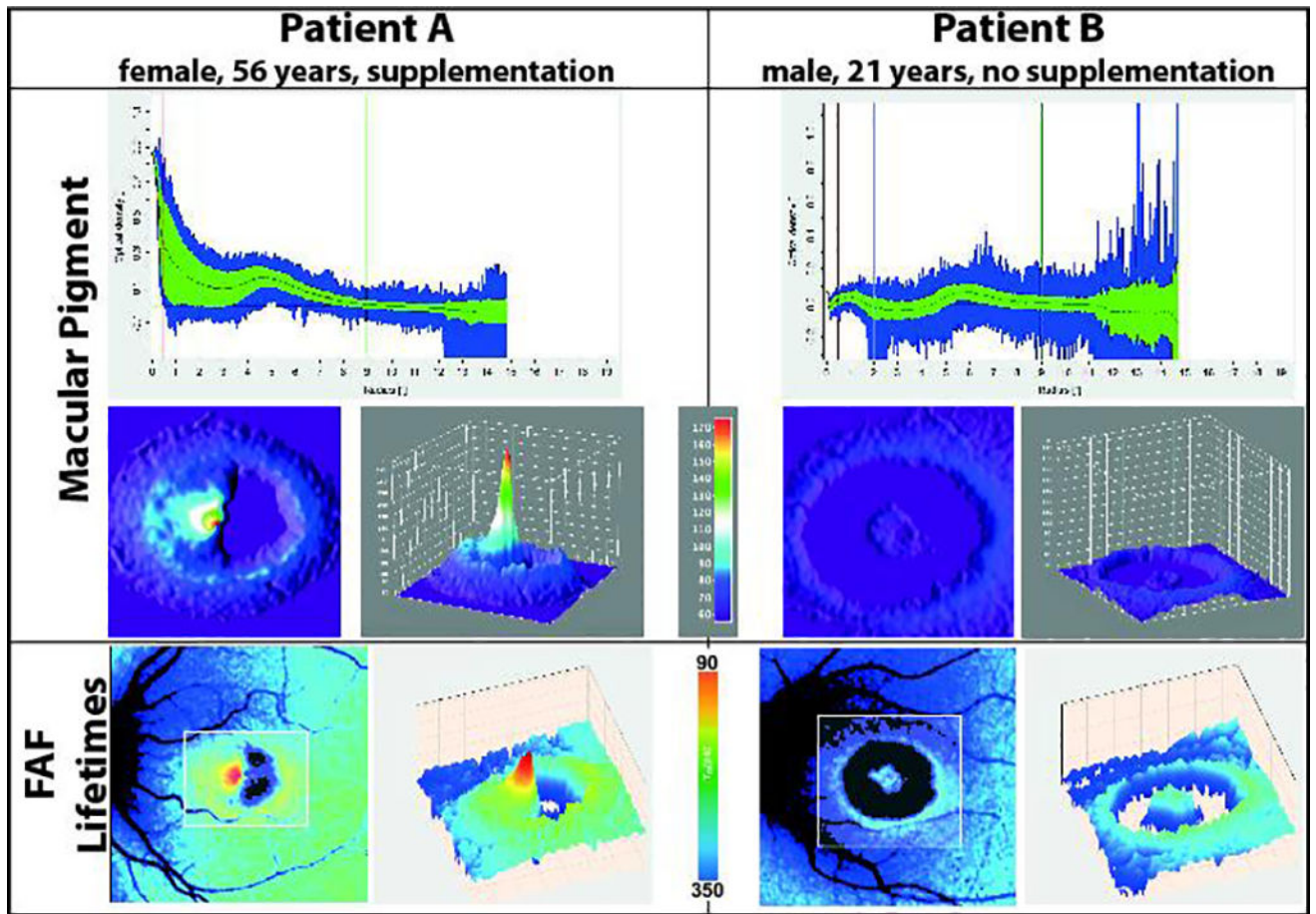


Figure 4. Macular pigment means and FAF lifetimes in two different patients with MacTel (A, B), one with zeaxanthin supplementation and the other without carotenoid supplementation.

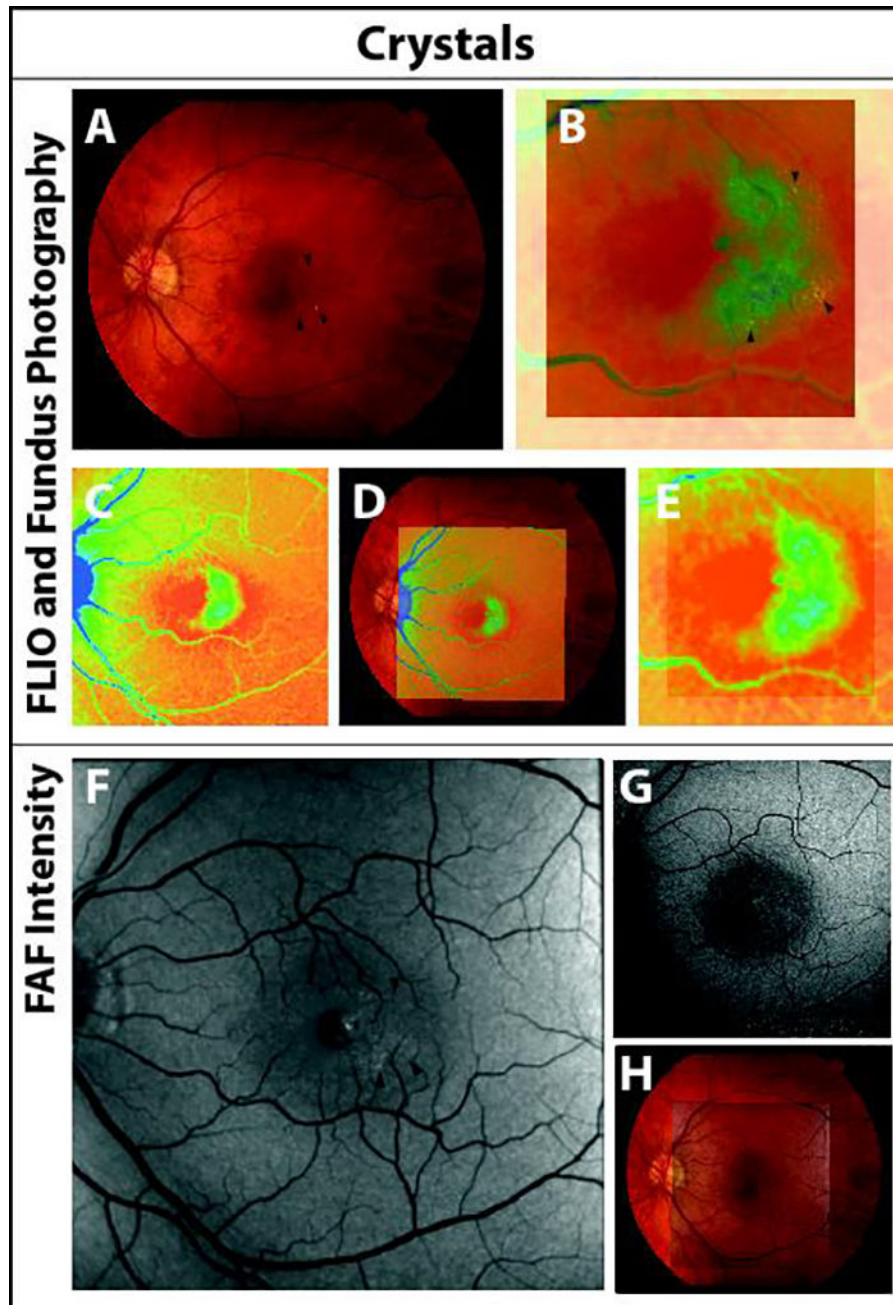


Figure 5. Fundus photography (A) and FAF lifetime image (C) as well as their overlay (B, D, E) showing crystals (arrows) within the prolonged FAF lifetimes at the MacTel area. Short spectral channel FAF intensity (498 – 560 nm, F) reveals crystals as compared to the long spectral FAF (560 – 720 nm, G). Overlay of SSC FAF intensity image and fundus photograph is shown in H.

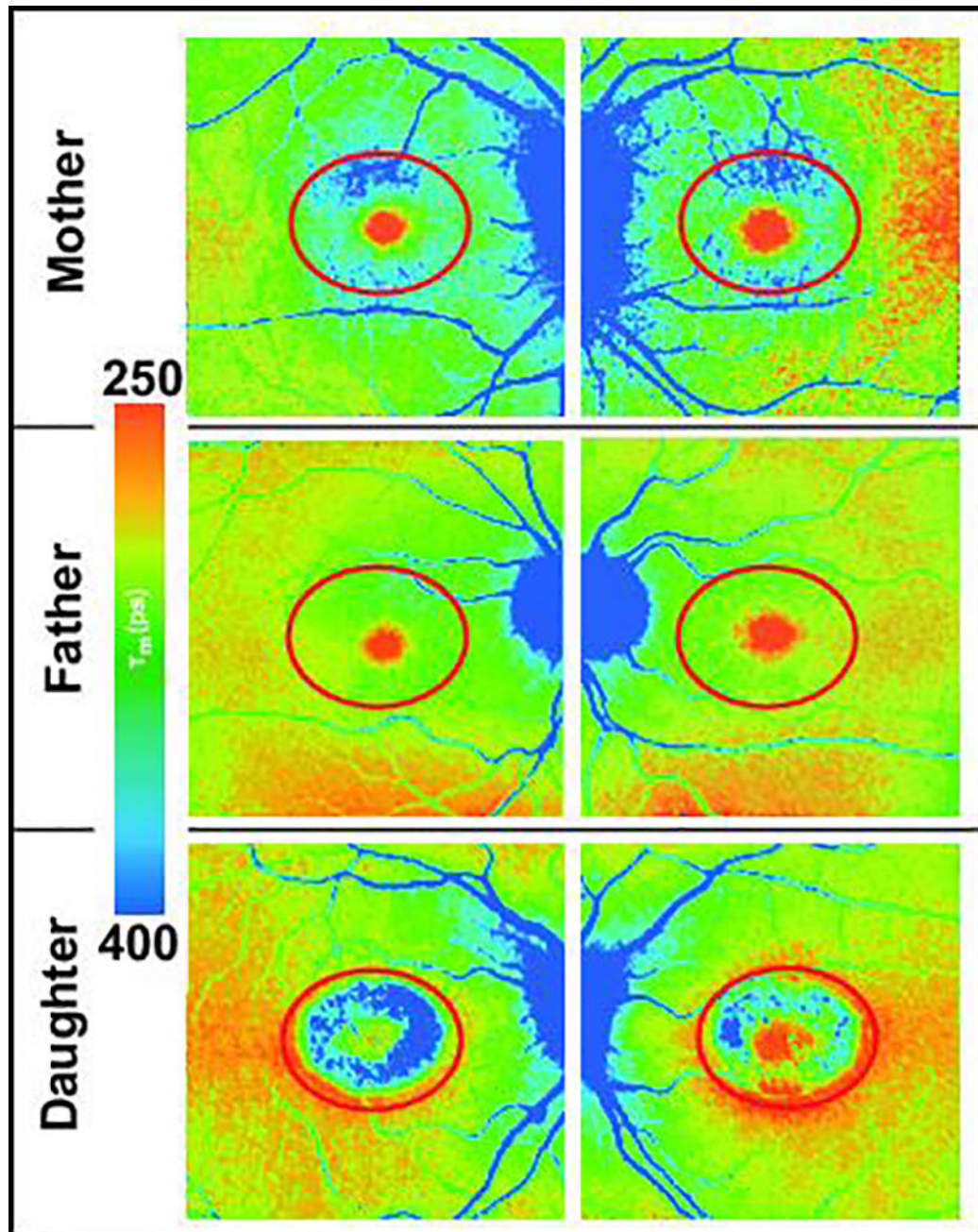


Figure 6.

Mean FAF lifetimes (SSC) of a family with MacTel. Whereas the daughter is strongly affected, both parents were clinically unaffected. The red oval demarcates the borders of the MacTel area. The FLIO images show unusually long mean FAF lifetimes inside the mother's and daughter's MacTel areas. The daughter's FAF lifetime ratios (T_2/T_1) were OD: 0.76 and OS: 0.81; the mother's were OD: 0.95 and OS: 0.93, and the father's were OD: 0.98 and OS: 0.99.

Table 1

Study Subjects

	MacTel	Healthy
Age	59.8 ± 13.6 years	60.1 ± 13.6 years
Subjects	42 eyes in 21 patients	42 eyes in 25 subjects
Gender	10 female (48 %); 11 male (52 %)	14 female (56 %); 11 male (44 %)
IOL	5 eyes (12 %)	6 eyes (14 %)
Stage	Number of MacTel eyes	
Early	12 Eyes	
Intermediate	6 Eyes	
Advanced	18 Eyes	
Foveal atrophy	6 Eyes	

Characterization of investigated groups. Stages of MacTel are explained within the Results section under “Subjects”.

Table 2

FAF Lifetimes in MacTel and Healthy Populations

	MacTel (All)	MacTel (Early)	Healthy
T2	312 ± 69 ps	312 ± 72 ps	301 ± 73 ps
T1	382 ± 81 ps	388 ± 76 ps	298 ± 84 ps
C	313 ± 68 ps	287 ± 71 ps	220 ± 81 ps
N1	355 ± 73 ps	345 ± 71 ps	312 ± 48 ps

FAF lifetimes (498 – 560 nm) in specific regions of interest (ROI) for all MacTel (n = 42), early MacTel (n = 12) and healthy subjects (n = 42).